JOURNAL OF RAMAN SPECTROSCOPY
J. Raman Spectrosc. 2008; **39**: 972–984
Published online 31 March 2008 in Wiley InterScience
(www.interscience.wiley.com) DOI: 10.1002/jrs.1940

JRS

A comprehensive micro-Raman spectroscopic study of prehistoric rock paintings from the Sierra de las Cuerdas, Cuenca, Spain

Antonio Hernanz,[1]* José M. Gavira-Vallejo,[1] Juan F. Ruiz-López[2] and Howell G. M. Edwards[3]

[1] Departamento de Ciencias y Técnicas Fisicoquímicas, Facultad de Ciencias, Universidad Nacional de Educación a Distancia (UNED), Senda del Rey 9, E-28040 Madrid, Spain
[2] Departamento de Prehistoria y Arqueología, Facultad de Geografía e Historia, UNED, Senda del Rey 7, E-28040 Madrid, Spain
[3] Centre for Astrobiology and Extremophiles Research, Chemical and Forensic Sciences, School of Life Sciences, University of Bradford, Bradford BD7 1DP, UK

Received 13 November 2007; Accepted 18 January 2008

An extensive micro-Raman spectroscopic study of prehistoric paintings found in open air rock shelters at the Sierra de las Cuerdas (Cuenca, Spain) was carried out. *In situ* optical microscopy, petrological polarized light microscopy, scanning electron microscopy (SEM) and energy dispersive X-ray microanalysis (EDX) were used as auxiliary techniques. Haematite (α-Fe_2O_3) of three granular types was the pigment that was most frequently encountered alone and in admixture with non-stoichiometric iron oxyhydroxides. A white pigment, but rarely used, results from a combination of white earths (α-quartz, anatase, muscovite and illite) and calcined bones (apatite); the presence of calcined bones also appears frequently in the red pigmented pictographs. The presence of significant amounts of charcoal underlying the white paint is suggestive of previous sketching on the shelter walls. Accretions of whewellite and weddellite resulting from the activity of fungi or lichens (e.g. *Verrucaria nigrescens*) are present in the painting panels, and carotenoids from this biological colonization were detected on several pictographs. The crystallization of gypsum and barytes in spallating areas of the painted surfaces is associated with sandstone weathering processes. An unusual deterioration of the art work caused by electric welding splashes resulting from the erection of protective ironwork grilles around the rock art panels was also detected.

Supplementary electronic material for this paper is available in Wiley InterScience at http://www.interscience.wiley.com/jpages/0377-0486/suppmat/

KEYWORDS: Raman microscopy; SEM/EDX; rock art; pigment; prehistoric paintings

INTRODUCTION

Currently, 42 open air rock shelters containing paintings are known in the Serranía de Cuenca range in Spain. The largest numbers of these, comprising 40 rock shelters with around 1000 pictographs, are located in the southern part of the range, called the Sierra de las Cuerdas, mainly located in the Villar del Humo municipality (Cuenca). A preliminary study by Raman microscopy of several significant prehistoric paintings from one of these rock shelters[1] has already been undertaken and forms the basis of the more comprehensive work described here, which includes selected rock shelters of archaeological significance: Marmalo III, Marmalo IV, Peña del Escrito II, Selva Pascuala (Figs 1–4) and Cueva del Tío Modesto.[1,2] Pictographs, accretions, substrata and alterations observed in these shelters have been studied in detail to identify the pigment palette composition and to determine the nature and origin of the accretions and alterations detected. The results will provide basic information on the technologies used by the prehistoric artists and are very important for the assessment of the dating and conservation of the paintings.[1,3] The discovery of whewellite- and weddellite-forming crusts that extend over a painted panel in one of these shelters[1,2] suggests an interesting possibility for radiocarbon dating of the art work as has been demonstrated

*Correspondence to: Antonio Hernanz, Departamento de Ciencias y Técnicas Fisicoquímicas, UNED, Senda del Rey 9, E-28040 Madrid, Spain. E-mail: ahernanz@ccia.uned.es

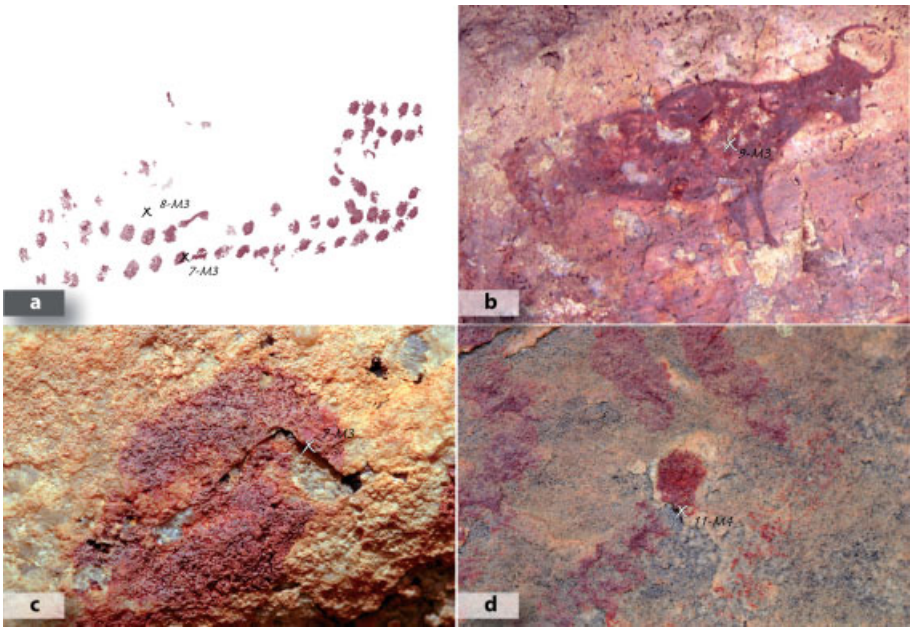

Figure 1. Some pictographs from the Marmalo III and Marmalo IV shelters indicating the sampling points: (a) digital reproduction of the finger dots 45 (pigment and accretion samples 7-M3 : 045 and 8-M3:sus respectively); (b) photograph of the bull 118 (pigment sample 9-M3 : 118); (c) microphotograph of the sampled finger dot (7-M3 : 045); (d) microphotograph of the serpentiform pictograph 26 at the Marmalo IV shelter (11-M4 : 026).

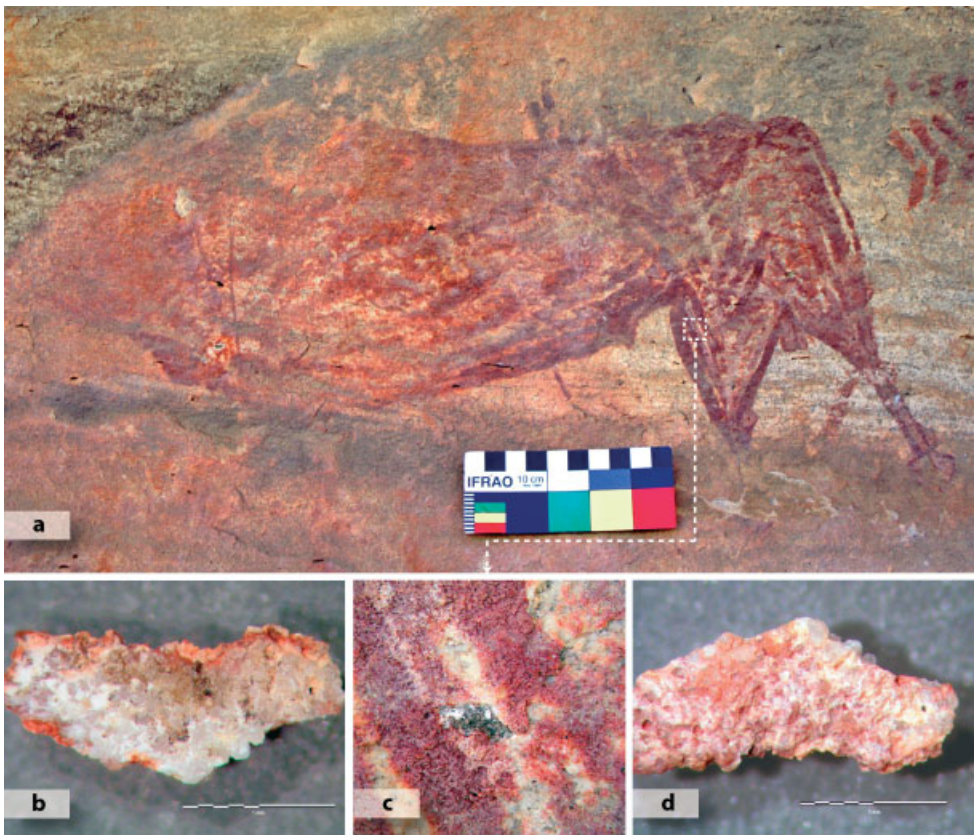

Figure 2. (a) Photograph of the bull 15 at the Marmalo IV shelter, the standard IFRAO coloured scale is 10 cm in length. The place where the sample of white pigment 10-M4 : 015 was taken is indicated. (b) Internal and (d) external faces of the sample 10-M4 : 15, the scales are 1 mm in length. (c) Microphotograph of the sampled location taken after the extraction of the sample. Black particles appear scattered over the substratum.

DOI: 10.1002/jrs

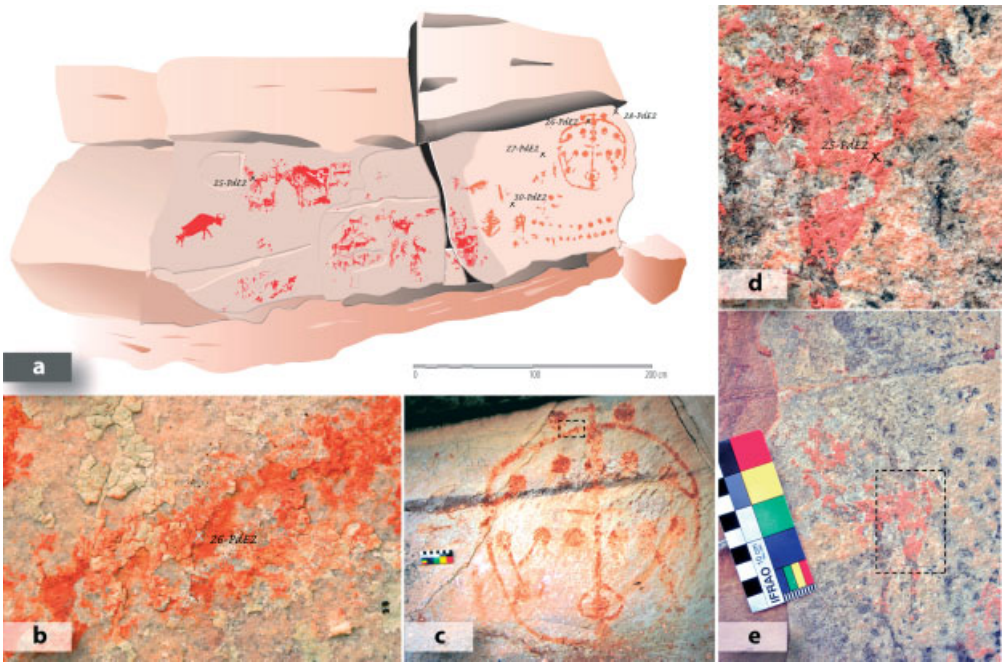

Figure 3. (a) Digital reproduction of the painting panel at the Peña del Escrito II shelter indicating the sampling points. The scale is 200 cm in length. (b) Microphotograph of the trace of pigment from which the sample 26-PdE2 : 112 was extracted. It corresponds to the area marked with a rectangle in (c) the circular motif 112. (d) Microphotograph of the position of the sample of pigment 25-PdE2 : 023 from the (e) goat 23.

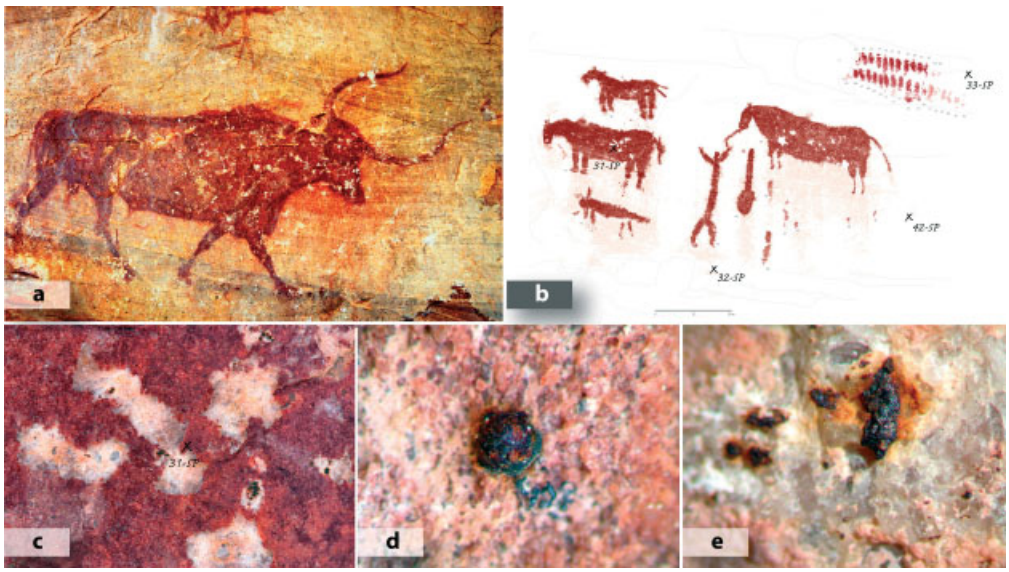

Figure 4. Images from the Selva Pascuala shelter. (a) Photograph of the bull 25 (SP:025). (b) Digital reproduction of one of the painting panels with the sampling points. The scale is 20 cm in length. (c) Microphotograph of the position of the sample of pigment 31-SP:041 from the horse 41. Microphotographs (d) and (e) of the black spots 41-SP : alt and 42-SP : alt, respectively, from the surface of the painting panels.

by the first radiocarbon ^{14}C accelerator mass spectrometry (AMS) dating of oxalate crusts related to Spanish prehistoric rock art.[4] Therefore, an additional objective of this work is to determine the stratigraphic relationship between any detected oxalate crusts and the pictographs, from which a reliable dating protocol could be established.[5–10] Another objective is to obtain information on the biogeological origin of these oxalate crusts. A white pigment has been used in a significant pictographical motif, as illustrated in Fig. 2. White pigments are generally quite exceptional in prehistoric

paintings, and therefore it is important to determine the composition and origin of this pigment in this prehistoric art work.

Archaeological background

Representative paintings of the rock art at Villar del Humo are located at the Peña del Escrito, Selva Pascuala and Marmalo sites, each one associated with several rock shelters. According to the ^{14}C AMS dating carried out in one of the shelters[4] of this range, it is believed that they were painted from the middle of the VIth millennium B.C. to the end of the IIIrd millennium B.C. During this time, several pictorial traditions were adopted in this mountain range, but all these preserved unaltered the main ideas of the authors of the oldest paintings, in which hunter-gatherers inseparably linked their subsistence and symbolic needs. With the transformations in their way of life through the adoption of herding and agriculture, the artists incorporated new designs into the older paintings in different styles. The result of this process is reflected today in the co-existence of the naturalistic (Levantine style) and schematic (Schematic style) pictographs in neighbouring shelters, or even encountered in the same pictorial panels.

Good examples of this complex process are found in the sites of Peña del Escrito II, Selva Pascuala, Marmalo III, Marmalo IV and Cueva del Tío Modesto. Natural representations of bulls, wild goats, deer, does and boars interacting with men, who are sometimes armed with bows and arrows, fill the panels, which are mainly painted in reddish colours. Sometimes, they are accompanied by groups of serpentiform designs, dotted and dashed lines, or schematic anthropomorphs that often add to the previous scenes without disturbing them. Some of these pictographs are acknowledged to be among the best preserved and better executed in Mediterranean Spain: for example the large bulls from Selva Pascuala (Fig. 4) and Marmalo III (Fig. 1), or the goats from Peña del Escrito II (Fig. 3).

EXPERIMENTAL

A comprehensive description of the experimental protocol followed in our study of these prehistoric paintings by *in situ* optical microscopy, sampling by excision, Raman microscopy and the development of the Micr-Art database has been given elsewhere.[1,2,11] Particular details of the present study are given below. Microphotography of archaeologically significant parts of the painting panels and pictographs by *in situ* optical microscopy assisted in the selection of the sampling points. Rock shelters, pictographs, accretions and their substrata were selected for sampling according to the criteria of archaeological relevance, their state of conservation and the specific irregularities of the rock surface. The samples were numbered according to a code established for the Micr-Art database.[1] Two motifs were sampled in the painting panel of the Marmalo III rock shelter: the finger dots 45 and the bull 118 (samples 7-M3 : 045 and 9-M3 : 118, respectively), Fig. 1(a), (b), (c). A sample of the accretion (8-M3:sus) on the painting panel of this shelter was also extracted, Fig. 1(a). Samples of the serpentiform pictograph 26 (11-M4 : 026), Fig. 1(d), and of the white pigment from the bull 15 (10-M4 : 015), Fig. 2, located in the Marmalo IV shelter were obtained, together with a spallated sandstone flake with adherent accretions (50-M4:sus). To elucidate the origin of the white pigment used in the pictographs, up to 12 samples of different white earths from the surrounding area were collected. The goat 23 (25-PdE2 : 023), Fig. 3(a), (d), (e), and the circular motif 112 (26-PdE2 : 112), Fig. 3(a), (b), (c), from the Peña del Escrito II shelter were also sampled. In the Selva Pascuala shelter, the horse 41 was sampled (31-SP:041), Fig. 4(b), (c). Two sandstone flakes, one below the anthropomorph 43 (32-SP:043) and another containing accretions (33-SP : alt), were removed, Fig. 4(b), as well as samples of black spots observed on the surface of the painting panels of this rock shelter (41-SP : alt and 42-SP : alt), Fig. 4(d), (e). A polished thin section (thickness 20 μm) of a flake of pigment from the deer 47 of the Cueva del Tio Modesto shelter (sample 15-CTM:047)[1,2] was prepared using a polyester resin matrix. This thin section was examined with a petrological microscope using polarized light to observe its microstratigraphy. A sample (12-CTM:077) of the orange line 77 from the painting panel 2 of this shelter had been analysed previously,[1] but an additional sample of this pictograph (83-CTM:077) was excised for the present study. Finally, an area of the crust observed in this shelter was also sampled (80-CTM : alt).[1,2] Haematite (99.8% Fe_2O_3) was purchased from Strem Chemicals, USA, in order to check the Raman spectral changes occurring with change in granularity.

The micro-Raman spectroscopic study of the samples were carried out with a Jobin Yvon LabRam-IR HR-800 spectrograph coupled to an Olympus BX41 microscope according to the procedure described elsewhere.[1,2,11] The 632.8 nm line, maximum nominal power of 700 μW, of a He–Ne laser was used for Raman excitation using effective powers of 315 μW (50× objective) and 286 μW (100× objective) measured at the sample position to avoid sample degradation.[12,13] The average spectral resolution in the Raman shift range of 100–1700 cm^{-1} was 1 cm^{-1} (focal length 800 mm, grating 1800 grooves/mm and confocal pinhole 100 μm). These conditions gave spectral footprints of ~1–2 μm (100× objective lens) and ~5 μm (50× objective lens) diameter at the specimen. A spectral integration time of between 2 and 480 s and up to 100 accumulations were used to achieve an acceptable signal-to-noise ratio. For regions of low fluorescence, an integration time of 30 s and 16 spectral accumulations were usually satisfactory but a 2 s integration time and 100 spectral accumulations were used for highly fluorescent sample regions. Wavenumber shift calibration was accomplished with 4-acetamidophenol, naphthalene and sulfur[14] standards over the range 150–3100 cm^{-1} and gave a mean deviation of $\Delta\nu_{cal} - \Delta\nu_{obs} = 0.43 \pm 0.16\ cm^{-1}$

DOI: 10.1002/jrs

($t_{Student}$ 95%). Baseline adjustment or spectral smoothing were not applied to the observed spectra. The software package GRAMS/AI v.7.00 (Thermo Electron Corporation, Salem, NH, USA) was used to assist with the wavenumber peak-picking procedure. A macroscopic FT-Raman spectrum of the sample of the white pigment 10-M4 : 015 was obtained using a Bruker RFS100 interferometer with a liquid-nitrogen-cooled Ge detector at 77 K. The line at 1064 nm of a Nd^{3+}/YAG laser with a nominal power of 100 mW at source was used for Raman excitation, and 2000 interferograms were accumulated with a spectral resolution of 4 cm^{-1}.

The micromorphology and distribution of the components in the samples were determined using a Hitachi S-3000N scanning electron microscope equipped with an Everhart–Hornley detector of secondary electrons with an operating resolution of 3 nm. X-ray microanalyses (EDX, dispersive X-ray microanalysis) of the samples were carried out with an energy dispersive X-ray spectrometer, Rontec Xflash Detector 3001, coupled to the scanning electron microscope, Peltier-refrigerated and with the Be window removed. The samples were previously coated with an Au/Pd alloy in a Polaron Range SC7620 sputter-coating instrument.

RESULTS AND DISCUSSIONS

Marmalo III

The Raman spectra of the samples from this shelter, 9-M3 : 118 and 7-M3 : 045, Fig. 5(a), (b), (e), indicate that the pigment used for the bull 118 and the finger dots 45 is haematite.[1–3,12,15,16] This is the red pigment generally used for the pictographs of the Sierra de las Cuerdas.[1,2] Strong bands of whewellite (calcium oxalate monohydrate) are also observed, Fig. 5(a), (b), (e), (f), (g). This oxalate is frequently found on rocks exposed to the atmosphere in the form of coatings and encrustations resulting from the metabolic activity of fungi and lichens.[1,2,17–28] We have observed that the haematite used in the paintings of the Sierra de las Cuerdas may be classified into three different granular types (Table 1), namely, <1 μm (fine), 1–10 μm (intermediate) and 20–100 μm (gross).[1] Fig. S1 (Supplementary Material) shows optical microphotographs of pigments with intermediate and fine granularity compared with the scanning electron microscopy (SEM) images of commercial haematite powder. This is an indication of the ability of the prehistoric artists to prepare pigments. The size of the haematite particles observed in the pigment of the bull 118 is 1–5 μm (9-M3 : 118) and it is 1–10 μm (7-M3 : 045) in the finger dots 45. They are therefore of the intermediate type and can be distinguished clearly using a 100× objective, Fig. S1(C) (Supplementary Material). A detailed study by Raman microscopy of these pigmented samples revealed the presence of other components. Three bands are observed at 1003, 1154 and 1510 cm^{-1} in different points of these samples, Fig. 5(c), (d), typical of a carotenoid.[22,25,26,28] The strong Raman bands at 1510 and 1154 cm^{-1} are predominantly due to the in-phase

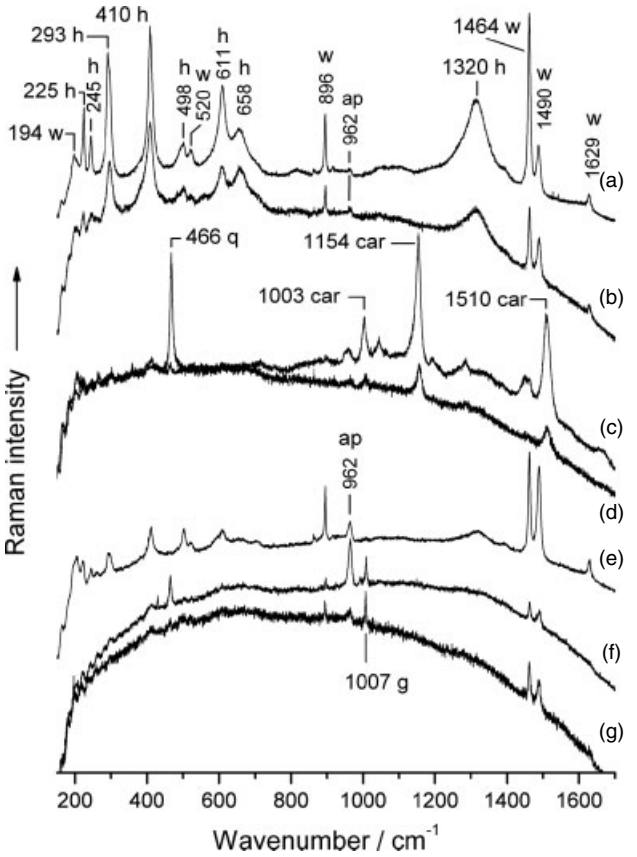

Figure 5. Raman spectra of representative points of the samples from the Marmalo III shelter: (a) 9-M3 : 118 pigment of the bull 118 showing bands of haematite, whewellite and traces of apatite; (b) 7-M3 : 045 pigment of a finger dot; (c) 7-M3 : 045 with typical bands of a carotenoid; (d) 9-M3 : 118 with bands of a carotenoid and α-quartz from the substratum; (e) 9-M3 : 118 showing bands of apatite, whewellite and haematite; (f) 7-M3 : 045 with bands of apatite, whewellite and gypsum; (g) 8-M3:sus accretion with whewellite and gypsum. Labels: w, whewellite; h, haematite; q, α-quartz; car, carotenoid; ap, apatite; g, gypsum.

C=C and C–C stretching modes ν_1 and ν_3 of the polyene chain, respectively, whereas the band of medium intensity at 1003 cm^{-1}, ν_6, is assigned to in-plane rocking modes of CH_3 groups attached to the polyene chain and coupled with C–C bonds.[29–31] It is difficult to determine precisely the specific carotenoid present in these samples from these wavenumber data alone; nevertheless, the wavenumber of the ν_1 band suggests that it should have a conjugated system of about 9–13 double bonds, with CH_3 groups attached.[29–31] Several carotenoids with similar Raman spectra could therefore be proposed: astaxanthine (1511, 1155 and 1006 cm^{-1}),[29] lycopene (1510, 1156 and 1008 cm^{-1}),[31] anhydrorhodovibrin (1513, 1152 and 1000 cm^{-1}) and spirilloxanthine (1509, 1151 and 998 cm^{-1}).[32,33] All these are deep red or purple-red pigments of biological origin. Lichens or photosynthetic bacteria (e.g. *Rhodospirillum rubrum*)[32] containing these carotenoids

DOI: 10.1002/jrs

Table 1. Results obtained from significant samples of pigments, substrata and alterations of prehistoric pictographs and painting panels of the Sierra de las Cuerdas

Sample/face	Colour	Components	Morphology	Traces
7-M3 : 045 pg./ext.	Red	Haematite, carotenoid, whewellite	h.c. 1 μm < ϕ < 10 μm	Gypsum, muscovite, anatase
8-M3:sus substratum/ext.	Ochre	Haematite, gypsum, whewellite	h.c. 1 μm < ϕ < 10 μm	
9-M3 : 118 pg./ext.	Red	Haematite, whewellite, carotenoid	h.c. 1 μm < ϕ < 5 μm	Apatite, gypsum, anatase, weddellite
/int.	Grey	α-Quartz, carotenoid	White crystals, black particles	Apatite, gypsum, magnetite, a. carbon, haematite
10-M4 : 015 pg./ext.	White, rose	α-Quartz, anatase, whewellite	q.c. $\phi \sim$ 100 μm h.c. 20 μm < ϕ < 100 μm	Muscovite, illite, haematite
/int.	White, black points, red edges	α-Quartz, anatase, muscovite, apatite, illite, a. carbon, haematite	q.c. ϕ > 100 μm a.c.f. 20 μm < ϕ < 100 μm	Gypsum, whewellite
11-M4 : 026 pg./ext.	Red	Haematite, whewellite, apatite	h.c. 1 μm < ϕ < 10 μm	a. Carbon, anatase, muscovite, α-quartz
/int.	White	α-Quartz	q.c. ϕ > 100 μm	
50-M4:sus substratum/ext	Pale ochre	Whewellite		
/int.	Grey	Gypsum		
25-PdE2 : 023 pg./ext.	Rose	Haematite, muscovite	h.c.1 μm < ϕ < 10 μm	Whewellite
/int.	Ochre	α-Quartz, haematite		Whewellite
26-PdE2 : 112 pg./ext.	Red	Haematite, apatite	h.c. ϕ < 1 μm	Whewellite
31-SP:041 pg./ext.	Red	Haematite, whewellite, barytes, gypsum, α-quartz	h.c. 1 μm < ϕ < 10 μm	Apatite, a. carbon
/int.	Rose	α-quartz, gypsum		
32-SP:043 pg./ext.	Rose	Haematite, whewellite, gypsum	h.c. 1 μm < ϕ < 10 μm	α-Quartz
/int.	Rose, brown spots	α-Quartz		Haematite
33-SP : alt alteration/ext.	Pale grey	Whewellite, weddellite, gypsum		Carotenoids, a. carbon, calcite
41-SP : alt alteration/ext.	Dark grey	Haematite, calcite	Metallic sphere with accretions	α-Quartz
42-SP : alt alteration/ext.	Black	Lepidocrocite		
12-CTM:077[a] pg./ext.	Orange, grey	Haematite, whewellite, α-quartz	h.c. ϕ < 1 μm q.c. $\phi \sim$ 100 μm	Weddellite, gypsum, a.h., a. carbon
/int.	Pale rose	α-Quartz	q.c. $\phi \sim$ 100 μm	Whewellite
13-CTM:122[a] pg./ext.	Red	Haematite, α-quartz, whewellite	h.c. 20 μm < ϕ < 100 μm	a. Carbon, weddellite
15-CTM:047[a] pg./ext.	Red	Haematite, α-quartz, gypsum	h.c. 20 μm < ϕ < 100 μm	Whewellite

(*continued overleaf*)

DOI: 10.1002/jrs

Table 1. (*Continued*)

Sample/face	Colour	Components	Morphology	Traces
15-CTM:047[b] thin section/sub.	Rose	α-Quartz, haematite	h.c. 20 μm < ϕ < 100 μm	Muscovite, microcline, anatase, rutile
/acc.-pg.-acc.	White-red-white	Whewellite-haematite-whewellite	h.c. 20 μm < ϕ < 100 μm	Gypsum
16-CTM:129[a] pg./ext.	Greyish blue	Whewellite, α-quartz	h.c. 20 μm < ϕ < 100 μm q.c. $\phi \sim$ 100 μm	a. Carbon, haematite
/int.	Rose	Haematite, α-quartz	h.c. 20 μm < ϕ < 100 μm q.c. $\phi \sim$ 100 μm	
80-CTM : alt alteration/ext.	White	Whewellite	Fungal hyphae encrusted with calcium oxalate crystals.	
83-CTM:082 pg./ext.	Orange, grey	Haematite, a.h.	h.c. ϕ < 1 μm	Weddellite, whewellite, gypsum

[a,b] Refs 1,2, respectively. Abbreviations: a., amorphous; acc., accretion; a.c.f., amorphous carbon fragments; a.h., amorphous (non-stoichiometric) iron oxyhydroxides; ext., external face; int, internal face; h.c., haematite crystals; pg., pigment; q.c., α-quartz crystals; sub., substratum.

could possibly exist in these pigmented samples.[34,35] A strong Raman band at 466 cm^{-1} appears in many spectra, Fig. 5(d), (f), and can be assigned to the O–Si–O stretching vibration of α-quartz, the main component of the Triassic sandstone substratum[2] at these sites and an abundant mineral in this region. An interesting band at 962 cm^{-1} is assigned to the symmetric stretching mode of the tetrahedral phosphate anion $\nu_1(PO_4^{3-})$ of apatite $Ca_5(PO_4)_3(F,Cl,OH)$ in both samples.[36–38] Several hypotheses could be envisaged about the origin of this mineral, namely, native apatite included in the source of haematite used by the painters, the use of a bone tool for painting or grinding the haematite and, finally, the use of a recipe to prepare the pigment that includes powdered haematite and calcined bones. Phosphates have not been detected anywhere in the numerous samples of substrata analysed,[1,2] and is absent from the 12 samples of white earths from the surrounding area; the geological maps of the Sierra de las Cuerdas[39] do not indicate the presence of phosphates in this region. A detailed study of the traces left in the pictographs for the tool used to apply the pigment and associated artefacts in the cave does not confirm that bones were utilised for this purpose[40] and the sample 7-M3 : 045 actually corresponds to a finger dot. On the other hand, haematite is harder than apatite and the use of bone implements to grind the pigment is not appropriate. The presence of apatite in prehistoric paintings has been noted hitherto in France[41] and Spain.[42,43] Therefore, a pigment preparation recipe that includes haematite and calcined bone appears to be the most plausible hypothesis for the presence of phosphates in our specimens. As was observed previously,[1,2] the painting panels of the rock shelters at the Sierra de las Cuerdas are usually coated by accretions of whewellite and gypsum. The Raman spectra of the sample 8-M3:sus from this shelter, Fig. 5(g), show bands of whewellite and the strong band of gypsum at 1007 cm^{-1} due to the symmetric stretching mode of the tetrahedral sulphate anion, $\nu_1(SO_4^{2-})$.[15,20,36,37,44]

Marmalo IV

The spectra of the sample 11-M4 : 026, Fig. 6(a), (b), from the serpentiform design 26, Fig. 1(d), show that the pigment again contains haematite and apatite. The expanded scale of the spectral region around the apatite band at 962 cm^{-1} included in Fig. 6 illustrates more clearly the assignment of the observed bands. Traces of whewellite and gypsum are also detected here. The haematite microcrystals have an intermediate granularity, Fig. S1(C) (Supplementary Material) and Table 1. As was indicated previously, the surface of the painting panels is usually covered by accretions of whewellite and gypsum.[1,2] The sample of this accretion from the Marmalo IV shelter, 50-M4:sus, gives rise to Raman spectra, Fig. 6(c), (d), with very strong bands of whewellite and gypsum. Many painting panels are evidently suffering from sandstone flaking, which can be directly attributed to the crystallization of gypsum in the sandstone pores near the surface.[1,45,46] The results of the study of the white pigment used in the bull 15 pictograph of this shelter are described subsequently.

DOI: 10.1002/jrs

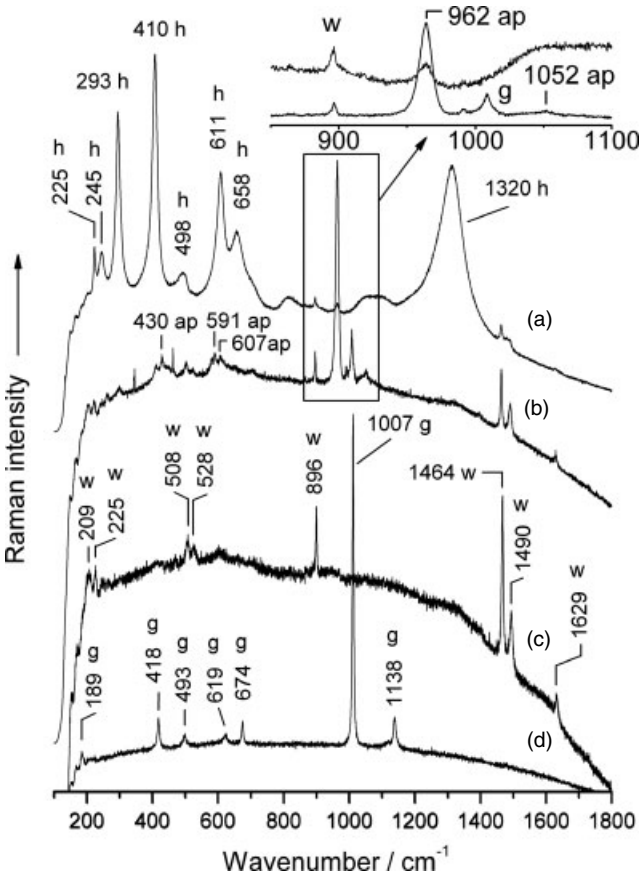

Figure 6. Raman spectra of representative points of samples from the Marmalo IV shelter: (a) 11-M4 : 026 pigment of the serpentiform pictograph 26 showing bands of haematite and traces of apatite and whewellite; (b) another point of this sample with stronger bands of apatite and additional bands of gypsum and whewellite; (c) 50-M4:sus external face of an accretion containing whewellite; (d) gypsum. Labels: h, haematite; ap, apatite; w, whewellite; g, gypsum.

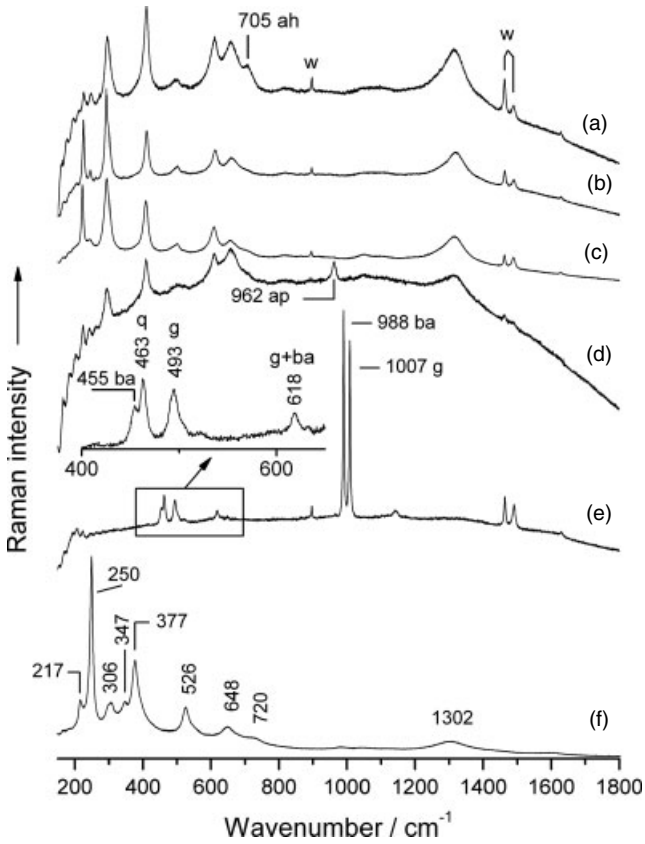

Figure 7. Raman spectra of representative points of the samples: (a) 83-CTM:077 pigment of the orange line 77 of the painting panel 2 at the Cueva del Tio Modesto shelter showing bands of haematite, whewellite and an additional band at 705 cm^{-1} assigned to amorphous iron oxyhydroxides; (b) 31-SP:041 pigment of the horse 41 from Selva Pascuala shelter with haematite and whewellite; (c) 25-PdE2 : 023 pigment of the goat 23 from the Peña del Escrito II shelter showing also haematite and whewellite bands; (d) 26-PdE2 : 112 pigment of the circular motif 112 of this shelter with haematite, apatite and traces of whewellite; (e) another representative point of the sample 31-SP:041containing barytes, gypsum, α-quartz and whewellite; (f) 42-SP : alt black spot on the painted surface of this shelter showing lepidocrocite bands. Labels: ah, amorphous iron oxyhydroxides; ap, apatite; ba, barytes; g, gypsum; q, α-quartz; w, whewellite.

Peña del Escrito II

The goat 23 (sample 25-PdE2 : 023), Fig. 3(a), (d), (e), and the circular motif 112 (sample 26-PdE2 : 112), Fig. 3(a), (b), (c), are painted with haematite, Fig. 7(c), (d). The granularity of the haematite particles of the circular motif 112 is so fine that they cannot be determined with the maximum magnification (objective 100×) available to our microscope, and therefore the particles must be smaller than 1 μm, Fig. S1(D) (Supplementary Material). However, the haematite particles of the goat 23 pictograph have only an intermediate granularity, Table 1. Muscovite and α-quartz are minerals detected in many samples as they are natural components of the substratum.[2] Apatite has been found mixed with haematite in the pigment of the circular motif 112, Fig. 7(d). It is important to note that this mixture has been detected in four different pictographs from various rock shelters.

Selva Pascuala

The horse 41, Fig. 4(b), (c) and sample 31-SP:041, was also painted with haematite, Fig. 7(b), comprising an intermediate particle granularity, Table 1. This sample also contains accretions of whewellite, gypsum and barytes,[47] Fig. 7(e). Although barytes, $BaSO_4$, is a well-known white pigment that was used much as such in later periods,[16] its presence in this sample should be associated rather with the crystallization process of sulphates in the sandstone surface of the flaking

DOI: 10.1002/jrs

areas.[1,2,46] Gypsum, barytes and α-quartz bands appear together in the spectrum, Fig. 7(e), of a point at which the horse pictograph is suffering significant flaking, Fig. 4(c). Hence, gypsum and barytes must be considered as accretion or alteration products of the sandstone substratum. Part of the red pigment of the anthropomorph 43 has been transported downwards by rain; the sandstone flake 32-SP:043 extracted from this area, Fig. 4(b), contains haematite of intermediate granularity, Table 1. Another flake specimen (33-SP : alt) with accretions on the painting panel indicates that they too contain whewellite, weddellite and gypsum, Table 1, which are the usual components of the accretions observed in the painting panels of the Sierra de las Cuerdas.[1,2] Traces of carotenoids and amorphous carbon deposits suggest that the accretions of calcium oxalates could have been produced by lichens or bacteria. We have observed numerous black spots on the surface of these painting panels, Fig. 4(d), (e), some of them on the surface of the pictographs. The Raman spectra of samples of these spots (41-SP : alt and 42-SP : alt) reveal the presence of iron oxides and oxyhydroxides. Haematite has been identified, as well as lepidocrocite (γ-FeOOH),[12] Fig. 7(f). Many of these spots have a spherical shape, Fig. 4(d). A detailed study of these spots in different painting panels by *in situ* optical microscopy showed that most of them are composed of metallic spheres and particles, Fig. S2 (Supplementary Material), which in some cases have suffered atmospheric corrosion, Fig. 4(d), (e). The rock shelters at the Sierra de las Cuerdas containing paintings are protected from vandalism with iron grilles, and small metallic spheres similar to those identified in the black spots on the pictographs were found on these grilles. Therefore, we conclude that the protective grilles were set up using electric welding without protecting the underlying painting panels and that the black spots on the pictographs are the residues of electric welding splashes on the painting panels – a regrettable example of anthropic deterioration.

Cueva del Tío Modesto

The painting panel 2 of this shelter has been previously studied.[1,2,4] Nevertheless, the orange vertical lines are intriguing in composition and colour, and they form the object of significant archaeological interest. Although a sample of pigment (12-CTM:077) has been analysed hitherto,[1] these pictographs have been revisited and an additional sample was removed: 83-CTM:077. As established earlier,[1] the main component of the pigment is haematite of fine granularity, Fig. 7(a) and Table 1.

However, a spectral feature observed earlier[1] at $\sim$700 cm^{-1} in the sample 12-CTM:077 is enhanced in the new sample 83-CTM:077. A band at 705 cm^{-1} may be distinguished clearly in Fig. 7(a). Di-octahedral T-O-T (T = tetrahedral layer, O = octahedral layer) phyllosilicates common in the substratum (muscovite)[2] and soil (montmorillonite) have a strong Raman band[48] near 700 cm^{-1}. Muscovite,[48,49] $KAl_2(AlSi_3O_{10})(F,OH)_2$, exhibits a strong Raman band at $\sim$705 cm^{-1}, but its other two strong bands at 263 and 200 cm^{-1} do not appear in the spectra of both samples. Similarly, montmorillonite has[48,50] a strong band at 707 cm^{-1}, but its bands at 200 and $\sim$425 cm^{-1} are not observed in the spectra of the pigment. Maghemite, γ-Fe_2O_3, has an overlapping doublet[12,51] with peaks at 714 and 655 cm^{-1}, but it also has broad and very strong bands at 1378 and 1576 cm^{-1} and these are not detected in the spectra of the pigment. Non-stoichiometric (amorphous) iron oxyhydroxides, $FeO_x(OH)_{3-2x}$ ($x < 1$), give rise to a spectrum[52] with a broad band near 701 cm^{-1}; these amorphous oxyhydroxides could be present in the pigment, and would also contribute to its observed orange colour.

The microstratigraphy of the pigment layer corresponding to the deer 47 (15-CTM:047) may be distinguished in Fig. 8. Micro-Raman spectra indicate the stratigraphic composition of the observed layers: α-quartz from the substratum, an accretion of whewellite over it, haematite from the pigment, another whewellite crust and the gypsum microcrystals common in flaking areas.[1,2] Two pigment layers separated by oxalate accretions are observed in other regions; this could be due either to the superimposition of two pictographs or possibly to repainting processes. From these data, a time sequence of events on the rock surface has been suggested[2]; after a first lichen colonization of the sandstone, the prehistoric painters applied the pigment layer. Then a new lichen colonization covered the pigment with another oxalate layer. Finally, the crystallization of sulfates in the sandstone pores near the surface deposited the gypsum microcrystals. These microstratigraphic characteristics of the painting panel 2 have given rise to the first ^{14}C AMS dating of oxalate accretions associated with Spanish prehistoric rock art.[4] This technique cannot be applied directly to the pigment (α-Fe_2O_3); nevertheless, as the pigment is bracketed between oxalate layers of similar thickness, the results obtained should provide a reasonable approximation to the age of the paintings. The surface of the oxalate accretions in different shelters shows a morphology, e.g. Figure S3(A) (Supplementary Material), that resembles those generated by lichens.[2,18] In some cases, it is possible to find areas of the oxalate crusts (80-CTM : alt) in which colonies of lichens are still active. In these cases, Fig. S3(B) (Supplementary Material), it is possible to recognize fungal hyphae encrusted with oxalate microcrystals.[2] The EDX spectra of these microcrystals, Fig. S4 (Supplementary Material), confirm their composition; strong peaks of oxygen, calcium and carbon from calcium oxalates and weaker signals from the substratum (α-quartz, silicates and haematite) are observed.[2] A taxonomic study of samples of a black accretion from the ceiling and proximities of the painting panel 2 of Cueva del Tio Modesto shelter has identified the lichen *Verrucaria nigrescens* in these samples. The IR spectrum of one of these samples (12-CTM : alt) revealed a high content of whewellite.[1] For these reasons, and considering our previous

DOI: 10.1002/jrs

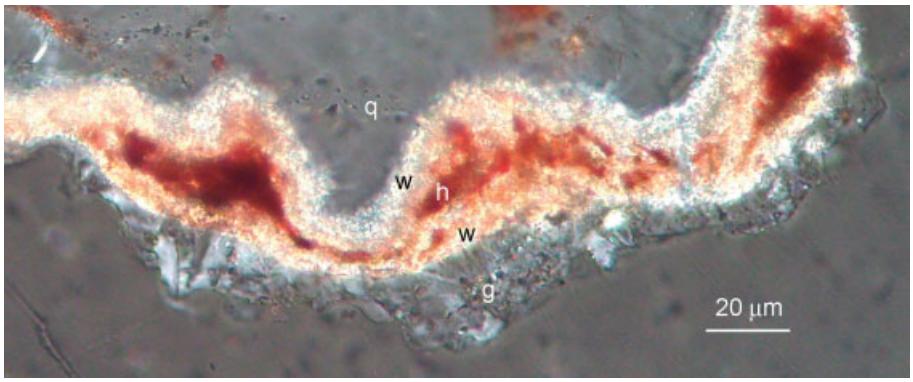

Figure 8. Microphotograph with polarized light of a thin section of pigment layer from the deer 47 (15-CTM:047) at the Cueva del Tío Modesto shelter illustrating the microstratigraphy. The layer of red pigment appears between layers of white oxalate microcrystals. The composition of the observed layers was identified by Raman microscopy: (q) α-quartz, (w) whewellite, (h) haematite, (g) gypsum.

results,[17–28] we can reasonably infer that the oxalate patinas found in the painting panels of the Sierra de las Cuerdas are the result of past fungal or lichen activity, some of which is still going on.

White pigment

The headless bull 15, Fig. 2, of the Marmalo IV shelter shows many white traces that reinforce the perception of the muscles in the red figure. This is one of the only two bichrome (red and white) pictographs found in the Sierra de las Cuerdas. This kind of figures is very rare, and even the white pigments alone are found in a limited number of figures from small geographical areas. Clay pigments (white earth) were used in Etruscan,[53] mediaeval and baroque paintings,[54] but information on prehistoric paintings is scarce and there is much interest in determining the composition of this pigment and its possible origin. A small sample, 10-M4 : 015, was removed from a leg of the bull between two red traces, Fig. 2(c). The excision of the sample revealed the presence of a significant number of black particles on the underlying sandstone substratum. Some of these particles are also observed at the internal interface of the sample, Fig. 2(b) and Fig. S5 (Supplementary Material). Their Raman spectra, Fig. 9(e), show the typical D1 and G bands of amorphous carbon[3,15,55,56] at 1342 and 1585 cm^{-1}, respectively, indicative of charcoal particles. The observation of these black particles found underneath the white pigment could be explained as remains of a previous sketch of the figure made by the artists using charcoal; the absence of any feature corresponding to a phosphate in the carbon spectrum excludes the possibility that the source of this charcoal is calcined bone and confirms its vegetable origin. The use of sketches made with charcoal in prehistoric pictographs was reported earlier in studies of prehistoric paintings in France.[57,58] The internal interface between the pigment and the substratum also shows red lines along the edges of the sample, Fig. 2(b), corresponding to parts of red traces from the pictograph, Fig. 2(c). Therefore, the layer of white pigment has been superimposed upon the red pigment. The Raman spectra of these red pigmented edges indicate that the red traces of the bull were painted with haematite, Fig. 9(f). The main component of the white pigment is α-quartz, Fig. 9(a). The microscopic images of the sample show many α-quartz crystals in contact or very close to each other,

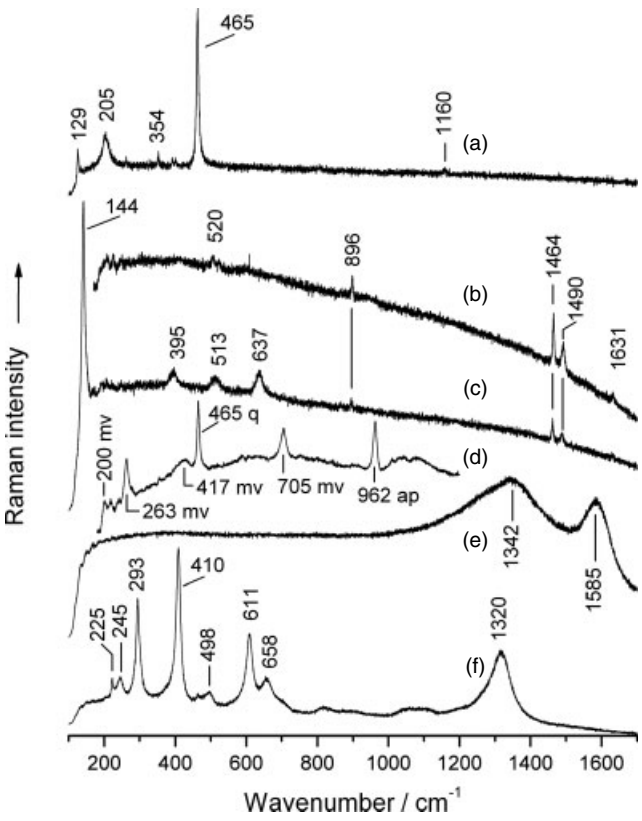

Figure 9. Raman spectra of components of the sample of white pigment 10-M4 : 015 from the bull 15, Fig. 2: (a) α-quartz; (b) whewellite; (c) anatase and whewellite; (d) apatite, muscovite and α-quartz; (e) amorphous carbon; (f) haematite. Labels: ap, apatite; mv, muscovite; q, α-quartz.

forming a microscopic mosaic. In the latter case, some type of cement seems to join these crystals. Very intense fluorescence is obtained when focusing the microscope onto the spatial regions containing these very small cement particles. In spite of these difficulties, significant numbers of anatase (TiO_2) particles have been identified,[59,60] Fig. 9(c), which contribute to the white colour of the pigment. This result is not surprising, as anatase is a component of the dominant rock in the region (Triassic sandstone)[2] and it has been found in several white earths from the surroundings, Table S1 (Supplementary Material). Nevertheless, it is curious that anatase, a synthetic pigment used nowadays and the source of an interesting controversy,[61,62] was nevertheless used, perhaps accidentally, in prehistoric art. The external face of the sample is partially covered by a crust of whewellite, Fig. 9(b): a common result in most samples. In an attempt to avoid the fluorescence by exciting the sample at 1064 nm in the near infrared, the corresponding FT-Raman spectrum of the sample, Fig. S6 (Supplementary Material), confirmed the previous micro-Raman results and did not reveal any additional components. However, by exciting at 632.8 nm it was possible to detect, Fig. 9(d), some particles of apatite, muscovite[48,49] and gypsum (not included in Fig. 9). It is relevant to note here that apatite has been discovered as an additional component of the red and white pigments in five pictographs from three different rock shelters. Therefore, the addition of calcined bones to the prehistoric pigments of the Sierra de las Cuerdas appears to be a repeated practice, probably related with some type of ritual. Like anatase, muscovite is frequently found in the Triassic sandstone,[2] but particles of this mineral from the mica group are much scarcer than the anatase particles in the white pigment. As pointed out above, the detection of gypsum microcrystals in this sample is another sign of the deteriorative effect on the paintings of the Marmalo IV shelter resulting in the sandstone flaking and spallation. The fluorescence observed when focusing the microscope on the cement micro-particles could be a sign of the presence of clay minerals, which is particularly pronounced with the laser excitation at 632.8 nm.[63] For this reason, we have used SEM/EDX techniques to locate possible clay minerals in these specimens. In the study of prehistoric pigments,[64,65] SEM images of the pigments show α-quartz crystals with accumulations of white microcrystals interspersed among them, Fig. S7(A) (Supplementary Material). Enlarged views revealed the plate-like morphology of these microcrystals stacked in the typical layer structure of sheet silicates,[66] Fig. S7(B) (Supplementary Material). The EDX spectra of the observed crystals correspond to α-quartz, Fig. S8(A) (Supplementary Material), and the sheet crystals contain Si, Al, O, K, Mg, Ca and Fe, Fig. S8(B) (Supplementary Material). Traces of calcium oxalates could contribute to the observed C and Ca signals. Kaolin-group minerals are common in the Sierra de las Cuerdas, but they cannot explain the presence of the Mg and Fe. Muscovite, previously detected in the sample, is in a similar situation. Nevertheless, typical clay minerals found in the region, e.g. illite and montmorillonite, could be good candidates and the EDX spectra of the sheet crystals correspond better to a micaceous mineral such as illite, which contains K and Fe, whereas Na, usual in montmorillonite, is not detected. On the other hand, illite is recognized as an alteration product of muscovite, a mica present in the sample. All the minerals identified in the white pigment are abundant in the Sierra de las Cuerdas. The analysis[2,15,48–50,67–69] of 12 white earths from the surroundings, Table S1 and Fig. S9 (Supplementary Material), indicates that the white sandstones (e.g. Ar1, Ar2 and Ar3) contain the dominant components of the pigment: α-quartz and anatase. Therefore, the pictographic pigment could be a natural mixture of minerals present in a white sandstone, but as we have not located the exact deposit of this white sandstone in the area, it is a distinct possibility that the prehistoric artists created their own mixture from small outcrops of white earths found nearby which may not exist today.

CONCLUSIONS

Haematite, α-Fe_2O_3, is the pigment generally used in the pictographs from the Sierra de las Cuerdas. This is a common red pigment in prehistoric paintings.[15,70–72] Three different types of granularity are observed: <1, 1–10 and 20–100 μm. The particle size ranges are similar to those found in pictographs at other sites.[71] Non-stoichiometric (amorphous) iron oxyhydroxides mixed with haematite have also been detected in one pictograph. The addition of calcined bones to haematite in order to prepare the red and white pigments appears to be an established practice, which is possibly suggestive of a ritual. It is important to note that no organic binders have been detected, but a mineral cement with anatase, muscovite and a micaceous clay such as illite has been found in this white pigment. The main components of this infrequently used pigment are α-quartz and anatase. The high concentration of charcoal particles found underneath the white paint at the interface with the substratum could be explained as remains of a previous sketch of the pictograph. All the painting panels are covered by patinas or crusts formed by whewellite and weddellite[1,2] accretions. These hydrated forms of calcium oxalate are generally the result of the activity of fungi and lichens, and we note that the observed oxalate microstructures are similar to those produced by lichens. Fungal hyphae encrusted with small calcium oxalate crystals have also been detected in some of the painting panels. Colonies of the lichen *Verrucaria nigrescens* have been identified in the proximities of the paintings at the Cueva del Tio Modesto shelter. Their IR spectra revealed a high whewellite content.[1] Moreover, carotenoids from lichens or photosynthetic bacteria have been detected on some pictographs. The observed microstratigraphy of pigment

DOI: 10.1002/jrs

and oxalate layers has given rise to the first ^{14}C AMS dating of oxalate crusts related to Spanish prehistoric rock art.[3] Several painting panels are suffering serious deterioration. Crystallization of sulfates, such as gypsum and barytes, in the sandstone pores and near the surface of the substrate is associated with the flaking and spallation that is affecting the paintings. It is vital that these areas should be preserved from humidity.[1] Unfortunately, the installation of iron grilles to protect the paintings has provoked an anthropic deterioration: electric welding splashes have been discovered on the pictographs in the vicinity of the metal grilles. We anticipate that these results will assist the future conservation of these attractive examples of prehistoric rock art.

Supplementary material

Supplementary electronic material for this paper is available in Wiley InterScience at: http://www.interscience.wiley.com/jpages/0377-0486/suppmat/

Acknowledgements

The authors thank S. Martín (Dept. Física Matemática y Fluidos, UNED), Dr E.V. Gavrilenko (Dept. Ciencias Analíticas, UNED) and Dr Vicente Cortés Corberán (Instituto de Catálisis and Petroleoquímica, CSIC, Madrid) for assistance with SEM/EDX analyses, microscopic polarized light images and the FT-Raman spectra, respectively. We gratefully acknowledge financial support from the Vicerrectorado de Investigación of UNED and the European Regional Development Fund (ERDF). We also thank the Consejería de Cultura de la Junta de Comunidades de Castilla La Mancha for financial support and permission to take photographs and samples of the paintings and substrata of the archaeological site. This work was supported by the Ministerio de Educación y Ciencia, I + D project CTQ2005-08959/BQU.

REFERENCES

1. Hernanz A, Gavira-Vallejo JM, Ruiz-López JF. *J. Raman Spectrosc.* 2006; **37**: 1054.
2. Hernanz A, Gavira-Vallejo JM, Ruiz-López JF. *J. Optoelectron. Adv. Mater.* 2007; **9**: 512.
3. Hernanz A, Gavira-Vallejo JM, Ruiz-López JF. *J. Raman Spectrosc.* 2006; **37**: 492.
4. Ruiz JF, Mas M, Hernanz A, Rowe MW, Steelman KL, Gavira JM. *Int. Newslett. Rock Art* 2006; **46**: 1.
5. Russ J, Palma RL, Loyd DH, Boutton TH, Coy MA. *Quaternary Res.* 1996; **46**: 27.
6. Watchman AL. *Stud. Conserv.* 1991; **36**: 24.
7. Russ JW, Kaluarachchi WD, Drummond L, Edwards HGM. *Stud. Conserv.* 1999; **44**: 91.
8. Watchman AL. *Antiquity* 1993; **67**: 58.
9. Steelman KL, Rickman R, Rowe MW, Boutton TW, Russ J, Guidon N. In *ACS Symposium Series*, vol. 831, Jakes K (ed). Archaeological Chemistry, 2002; 22.
10. Watchman A, O'Connor S, Jones R. *J. Archaeol. Sci.* 2005; **32**: 369.
11. Hernanz A, Gavira-Vallejo JM, Ruiz-López JF. *Asian J. Phys.* 2006; **15**: 187.
12. de Faria DLA, Venâncio Silva S, de Oliveira MT. *J. Raman Spectrosc.* 1997; **28**: 873.
13. David AR, Edwards HGM, Farwell DW, de Faria DLA. *Archaeometry* 2001; **43**: 461.
14. ASTM Subcommittee on Raman Spectroscopy. *Raman Shift Frequency Standards: McCreery Group Summary (ASTM E 1840).* American Society for Testing Materials: Philadelphia, PA, 2005; http://chemistry.ohio-state.edu/~rmccreer/shift.html.
15. Edwards HGM, Newton EM, Russ J. *J. Mol. Struct.* 2000; **550–551**: 245.
16. Burgio L, Clark RJH. *Spectrochim. Acta, Part A* 2001; **57**: 1491.
17. Watchman AL. *Stud. Conserv.* 1991; **36**: 24.
18. Russ J, Palma RL, Loyd DH, Boutton TH, Coy MA. *Quaternary Res.* 1996; **46**: 27.
19. Seaward MRD, Edwards HGM. *J. Raman Spectrosc.* 1997; **28**: 691.
20. Edwards HGM, Drummond L, Russ J. *Spectrochim. Acta, Part A* 1998; **54**: 1849.
21. Edwards HGM, Drummond L, Russ J. *J. Raman Spectrosc.* 1999; **30**: 421.
22. Holder JM, Wynn-Williams DD, Rull Pérez F, Edwards HGM. *New Phytol.* 2000; **145**: 271.
23. Beazley MJ, Rickman RD, Ingram DK, Boutton TW, Russ J. *Radiocarbon* 2002; **44**: 675.
24. Frost RL, Weier ML. *J. Raman Spectrosc.* 2003; **34**: 776.
25. Edwards HGM, Seaward MRD, Attwood SJ, Little SJ, de Oliveira LFC, Tretiach M. *Analyst* 2003; **128**: 1218.
26. Edwards HGM, Newton EM, Wynn-Williams DD, Lewis-Smith RI. *Spectrochim. Acta, Part A* 2003; **59**: 2301.
27. Jorge Villar SE, Edwards HGM, Seaward MRD. *Spectrochim. Acta, Part A* 2004; **60**: 1229.
28. Jorge Villar SE, Edwards HGM, Seaward RD. *Analyst* 2005; **130**: 730.
29. Veronelli M, Zerbi G, Stradi R. *J. Raman Spectrosc.* 1995; **26**: 683.
30. Withnall R, Chowdhry BZ, Silver J, Edwards HGM, de Oliveira LFC. *Spectrochim. Acta, Part A* 2003; **59**: 2207.
31. Schulz H, Baranska M, Baranski R. *Biopolymers* 2005; **77**: 212.
32. Picorel R, Randall EH, Cotton TM, Seibert M. *J. Biol. Chem.* 1988; **263**: 4374.
33. Qian Pu, Saiki K, Mizoguchi T, Kazukimi H, Tokutake S, Ritsuko F, Yasushi K. *Photochem. Photobiol.* 2001; **74**: 444.
34. Laiz L, Hermosin B, Caballero B, Saiz-Jimenez C. *Aerobiologia* 2000; **16**: 119.
35. Krumbein WE, Brehm U, Gorbushina AA, Levit G, Palinska KA. In *Fossil and Recent Biofilms. A Natural History of Life on Earth*, Krumbein WE, Peterson DM, Zavarzin GA (eds). Kluwer Academic Publishers: Dordrecht, 2003; 1.
36. Herzberg G. *Molecular Spectra and Molecular Structure II. Infrared and Raman Spectra of Polyatomic Molecules*. Van Nostrand Reinhold: New York, 1945; 100, 167.
37. Degen IA, Newman GA. *Spectrochim. Acta, Part A* 1993; **49**: 859.
38. Wopenka B, Pasteris JD. *Mater. Sci. Eng., C* 2005; **25**: 131.
39. Instituto Geológico y Minero de España. *Mapa Geológico de España E. 1:50000, Villar del Humo*, 2nd series (1st edn). Servicio de Publicaciones, Ministerio de Industria: Madrid, 1975.
40. Ruiz-López JF. Ph D Thesis, *Las pinturas rupestres en la Serranía de Cuenca. Análisis, revisión y crítica del concepto de estilo en las manifestaciones plásticas postpaleolíticas*, Universidad Nacional de Educación a Distancia, Facultad de Geografía e Historia, Madrid, 2007.
41. Hameau P, Cruz V, Laval E, Menu M, Vignaud C. *L'Anthropologie* 2001; **105**: 611.
42. Chalmin E, Menu M, Altuna J. *MUNIBE (Antropol.-Arkeol.)* 2002; **54**: 33.
43. Gárate D, Laval E, Menu M. *L'Anthropologie* 2004; **108**: 251.
44. Berenblut BJ, Dawson P, Wilkinson GR. *Spectrochim. Acta, Part A* 1971; **27**: 29.
45. Doehne E. In *Natural Stone, Wheathering Phenomena, Conservation Strategies and Case Studies*, Siegesmund S, Weiss T, Vollbrecht A (eds). Geological Society: Special Publications 205: London, 2002 55.
46. Hosono T, Uchida E, Suda C, Ueno A, Nakagawa T. *J. Archaeol. Sci.* 2006; **33**: 1541.

47. Misra AK, Sharma SK, Lucey PG. *Appl. Spectrosc.* 2006; **60**: 223.
48. Rinaudo C, Roz M, Boero V, Franchini-Angela M. *Neues Jahrb. Miner. Monatsh.* 2004; **2004**: 537.
49. Wada N, Kamitakahara WA. *Phys. Rev. B* 1991; **43**: 2391.
50. Bishop JL, Murad E. *J. Raman Spectrosc.* 2004; **35**: 480.
51. Sousa MH, Tourinho FA, Rubim JC. *J. Raman Spectrosc.* 2000; **31**: 185.
52. Dünnwald J, Otto A. *Corros. Sci.* 1989; **29**: 1167.
53. Bellelli V. Il guerriero di Ceri. In *Il guerriero di Ceri, Tecnologie per far rivivere e interpretare un capolavoro della pittura etrusca su terracotta*, Guidi GF, Bellelli V, Trojsi G (eds). Enea: Roma, 2006.
54. Hradil D, Grygar T, Hradilová J, Bezdicka P. *Appl. Clay Sci.* 2003; **22**: 223.
55. Beyssac O, Goffé B, Petitet JP, Froigneaux E, Moreau M, Rouzaud JN. *Spectrochim. Acta, Part A* 2003; **59**: 2267.
56. Smith DC, Bouchard M, Lorblanchet M. *J. Raman Spectrosc.* 1999; **30**: 347.
57. Clottes J, Menu M, Walter P. *Bull. Soc. Prehist. Fr.* 1990; **87**: 170.
58. Menu M, Walter P. *Revue Technè* 1996; **3**: 11.
59. Ohsaka T, Izumi F, Fujiki Y. *J. Raman Spectrosc.* 1978; **7**: 321.
60. Ohsaka T. *J. Phys. Soc. Jpn.* 1980; **48**: 1661.
61. Clark RJH. *Anal. Chem.* 2004; **76**: 2423.
62. Vandenabeele P, Edwards HGM, Moens L. *Chem. Rev.* 2007; **107**: 675.
63. Frost R, Kloprogge T, Smith J. *Internet J. Vib. Spectrosc.* 1999; **3**(4): 2, [www.ijvs.com].
64. Chalmin E, Menu M, Vignaud C. *Meas. Sci. Technol.* 2003; **14**: 1590.
65. Vignaud C, Salomon H, Chalmin E, Geneste JM, Menu M. *L'Anthropologie* 2006; **110**: 482.
66. Liu W. *Wat. Res.* 2001; **35**: 4111.
67. Frost RL. *Clays Clay Miner.* 1995; **43**: 191.
68. Frost RL, Fredericks PM, Kloprogge JT, Hope GA. *J. Raman Spectrosc.* 2001; **32**: 657.
69. Freeman JJ, Wang A, Kuebler KE, Haskin LA. *Lunar and Planetary Science XXXIV*. Abstract #1676, Houston, Texas, 2003.
70. Zoppi A, Signorini GF, Lucarelli F, Bachechi L. *J. Cult. Herit.* 2002; **3**: 299.
71. Mortimore JL, Marshall LJR, Almond MJ, Hollins P, Matthews W. *Spectrochim. Acta, Part A* 2004; **60**: 1179.
72. Ospitali F, Smith DC, Lorblanchet M. *J. Raman Spectrosc.* 2006; **37**: 1063.

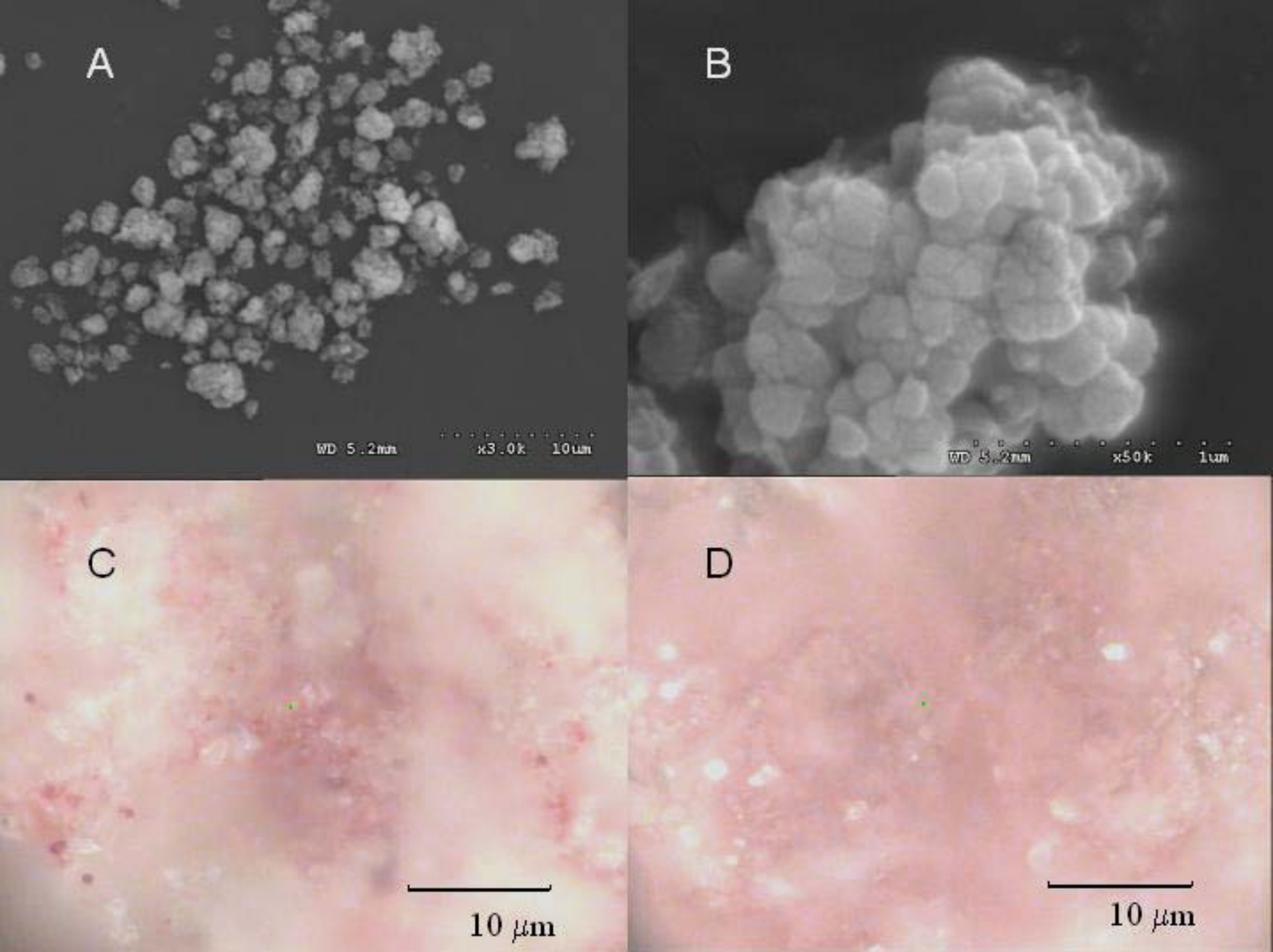
A
WD 5.2mm x3.0k 10um
B
WD 5.2mm x50k 1um
C
10 μm
D
10 μm


2 mm

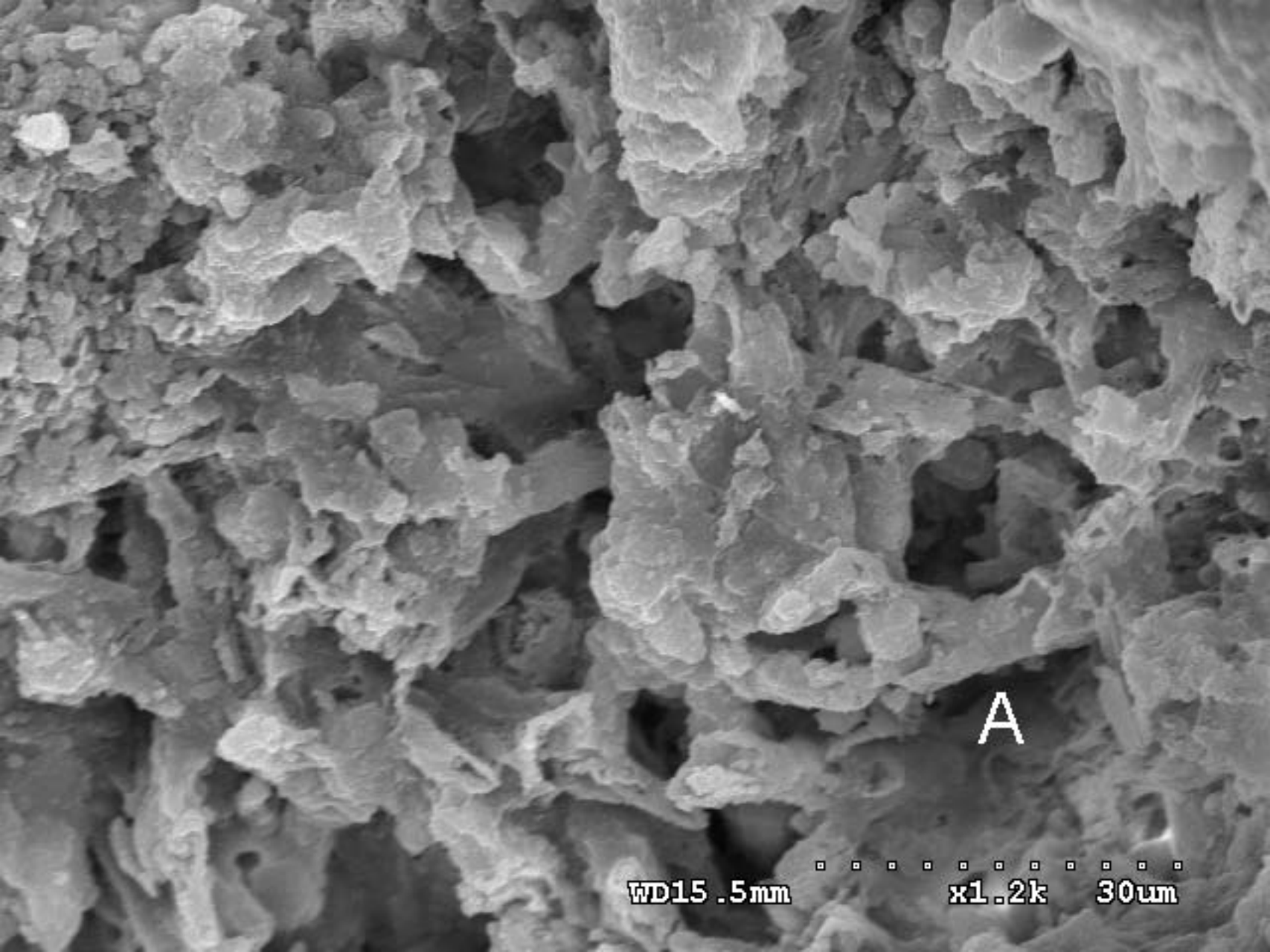
A
WD15.5mm
x1.2k
30um

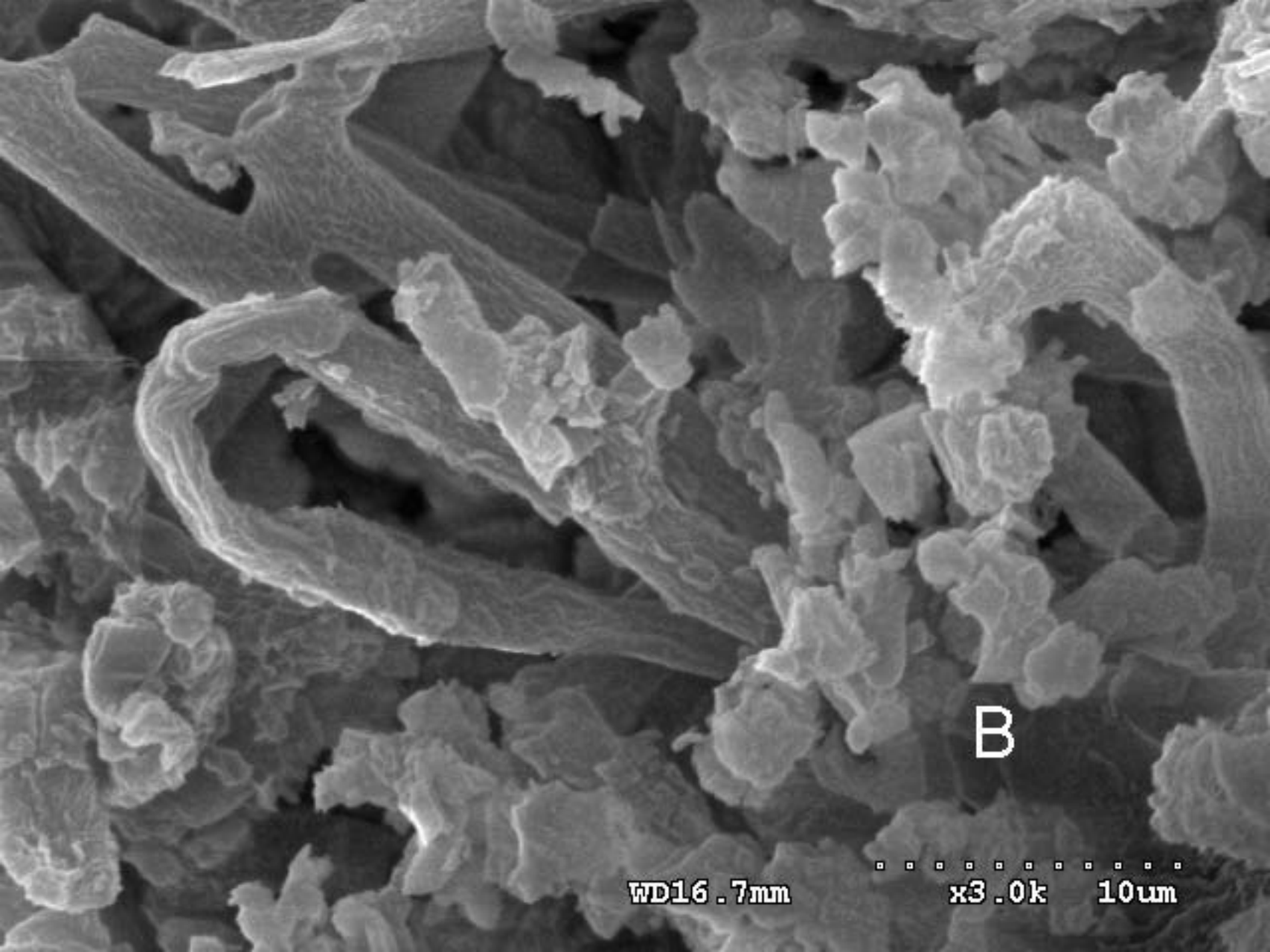
B
WD16.7mm
x3.0k 10um

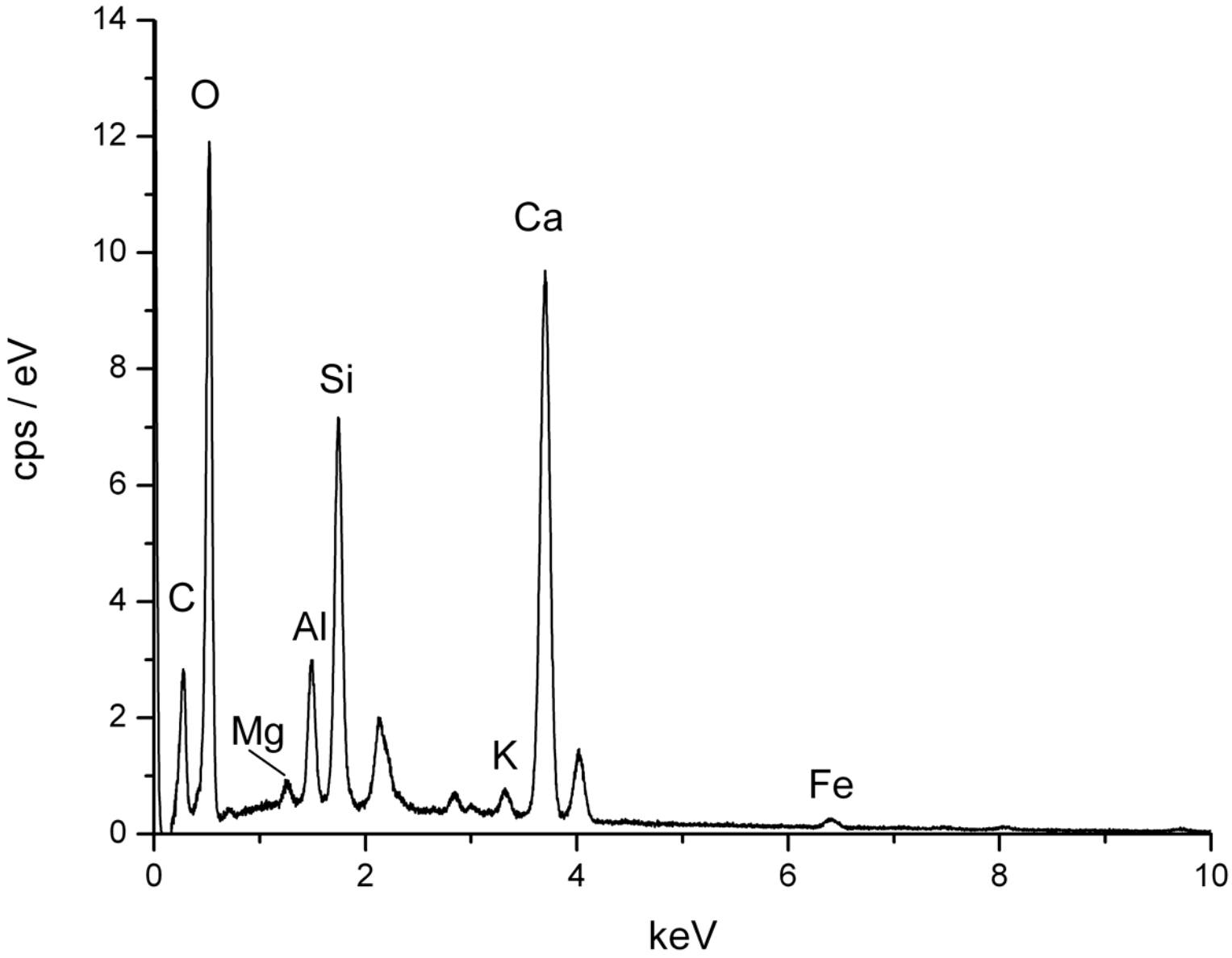
14
12
10
8
6
4
2
0
cps / eV
O
Ca
Si
C
Al
Mg
K
Fe
0
2
4
6
8
10
keV

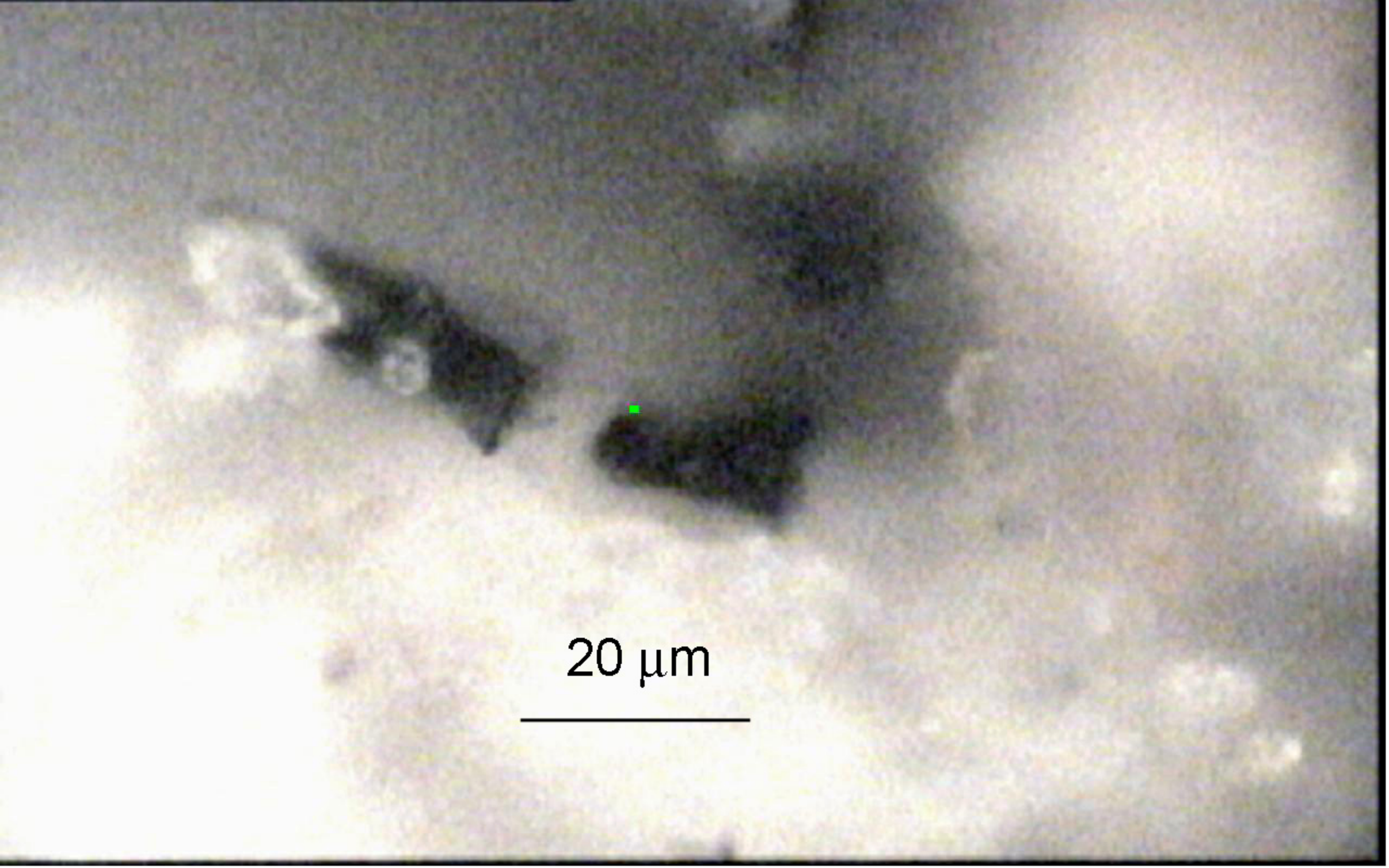
20 µm

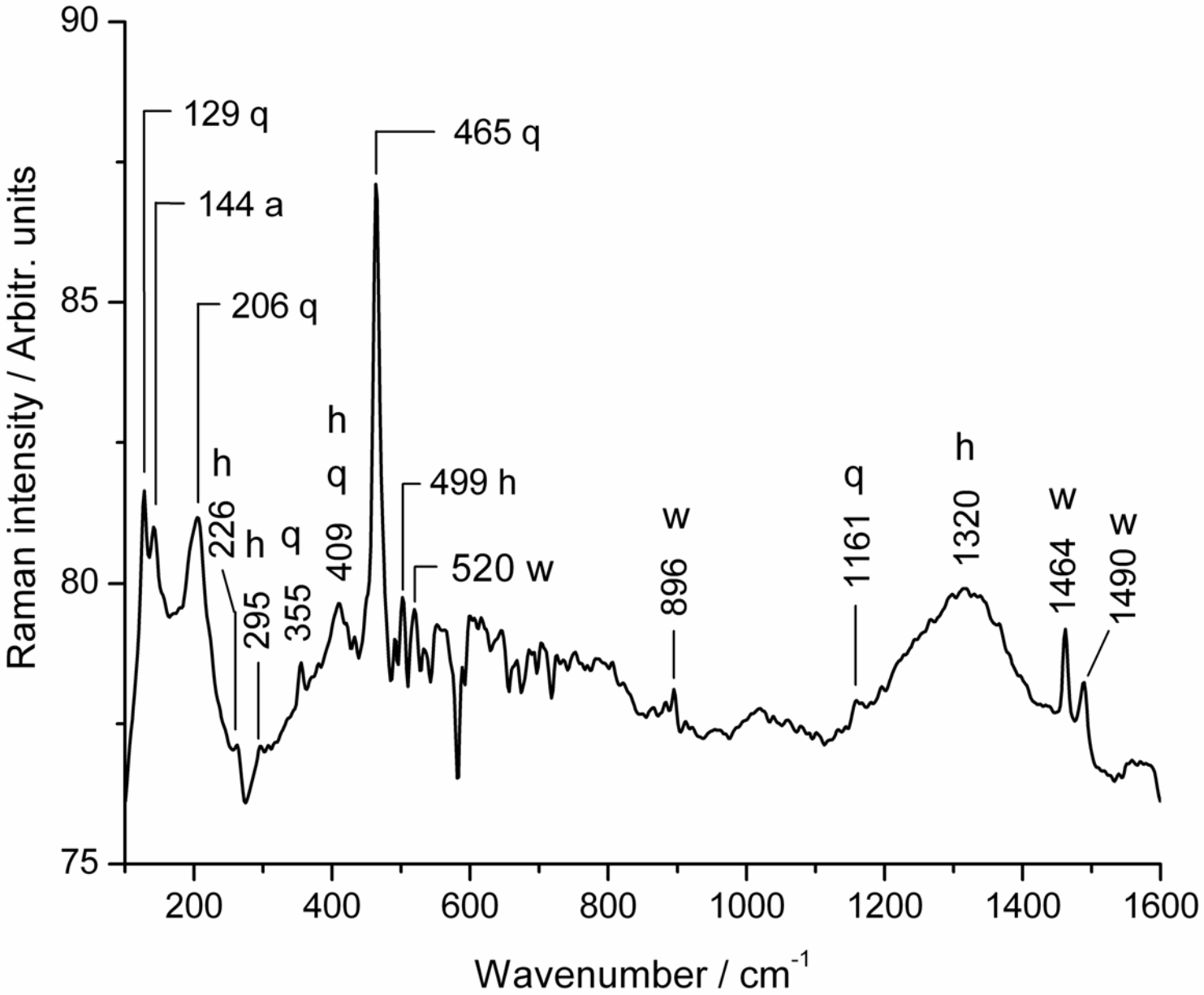
90
85
80
75
Raman intensity / Arbitr. units
200
400
600
800
1000
1200
1400
1600
Wavenumber / cm-1
129 q
144 a
206 q
226 h
295 h
355 q
409 q
465 q
499 h
520 w
896 w
1161 q
1320 h
1464 w
1490 w

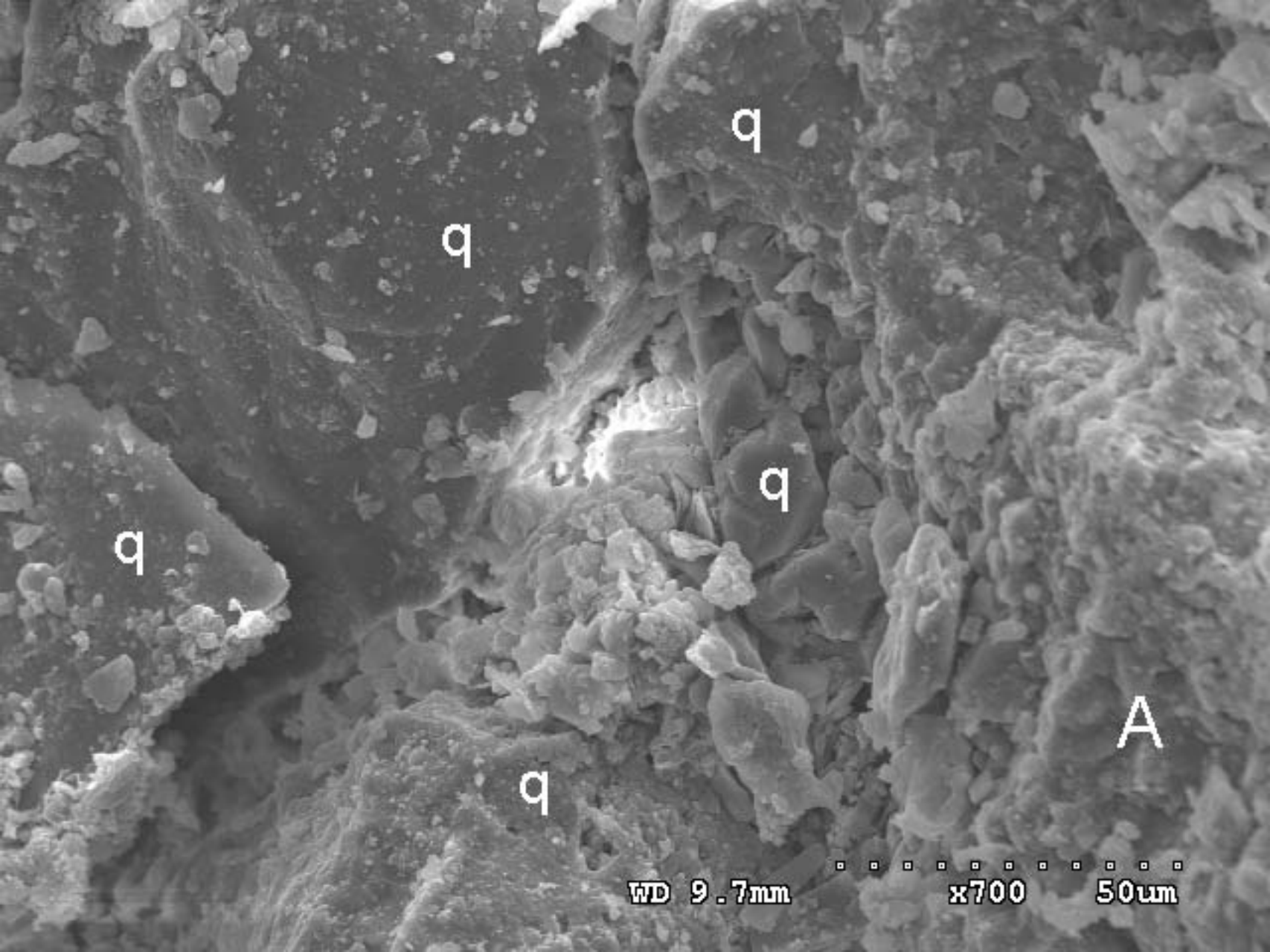
q
q
q
q
q
A
WD 9.7mm
x700
50um

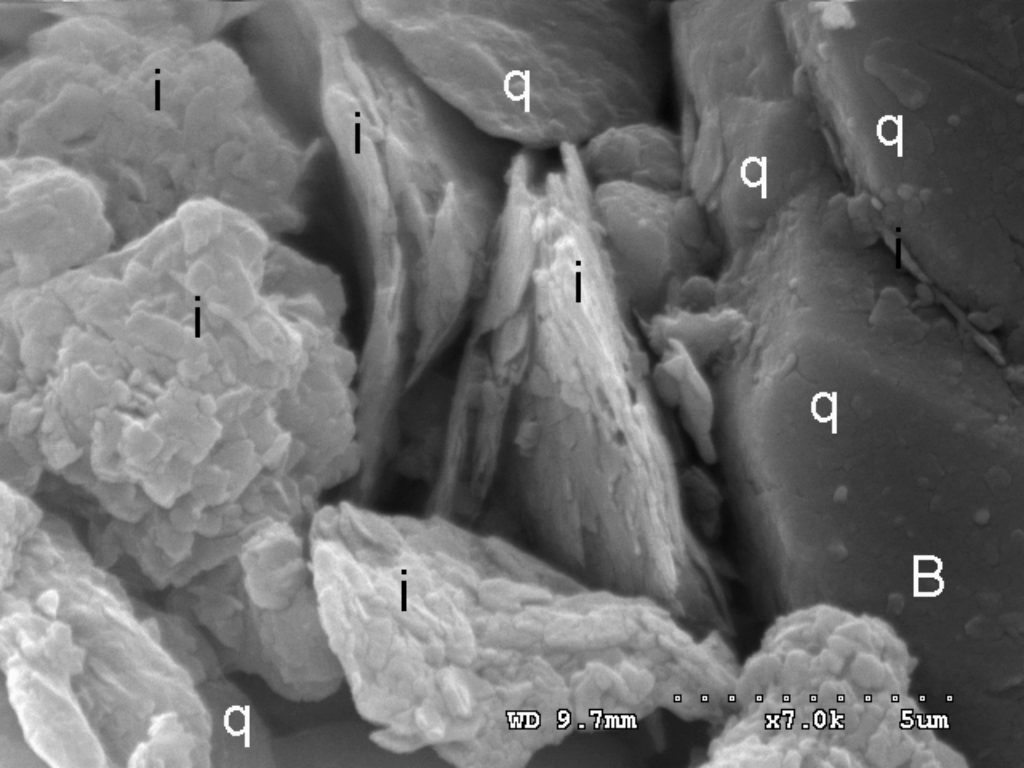
i
i
q
q
q
i
i
i
q
B
i
q
WD 9.7mm
x7.0k
5um

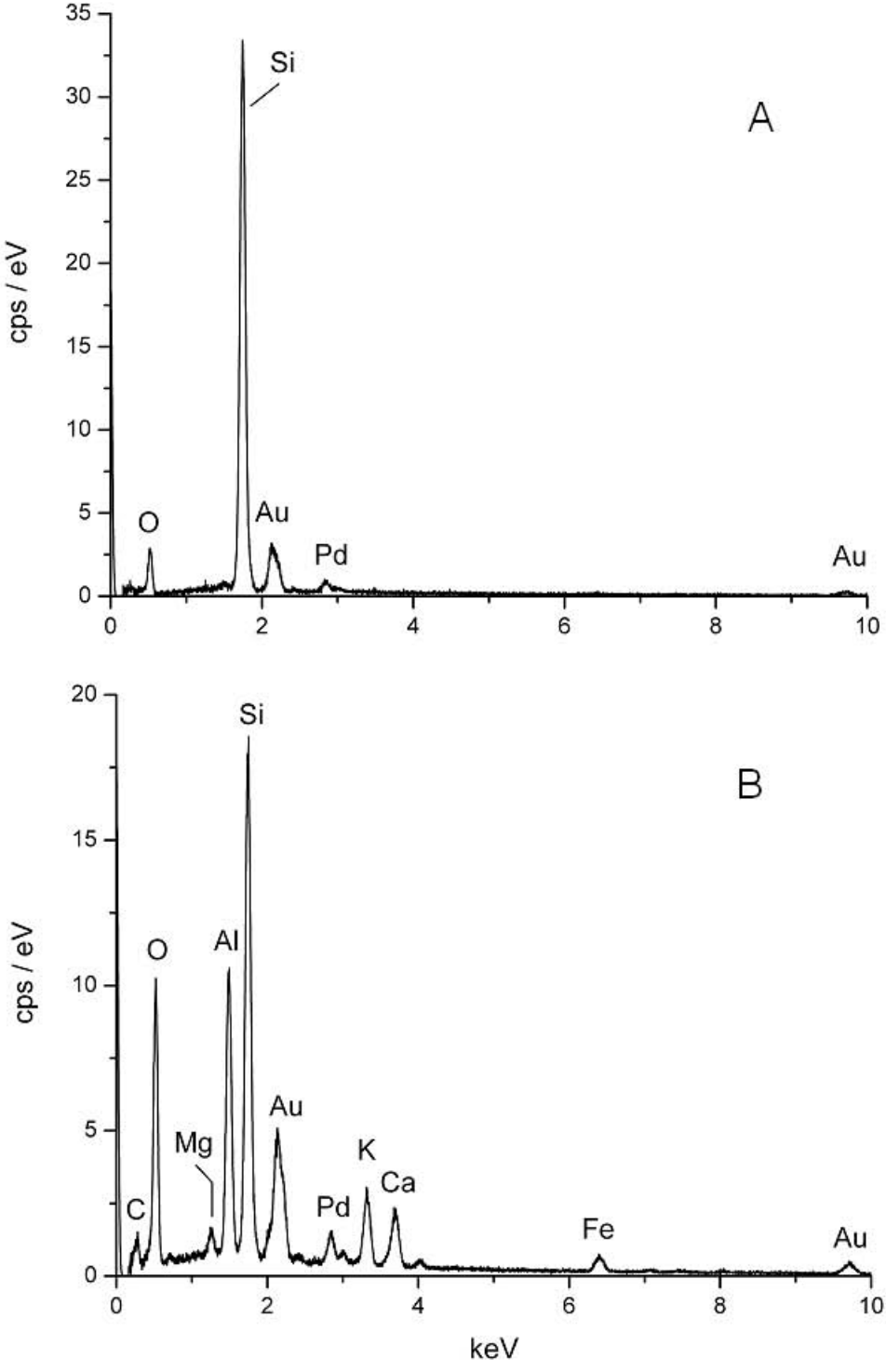
A
Si
O
Au
Pd
Au
cps / eV
B
Si
O
Al
Au
Mg
K
Ca
C
Pd
Fe
Au
cps / eV
keV

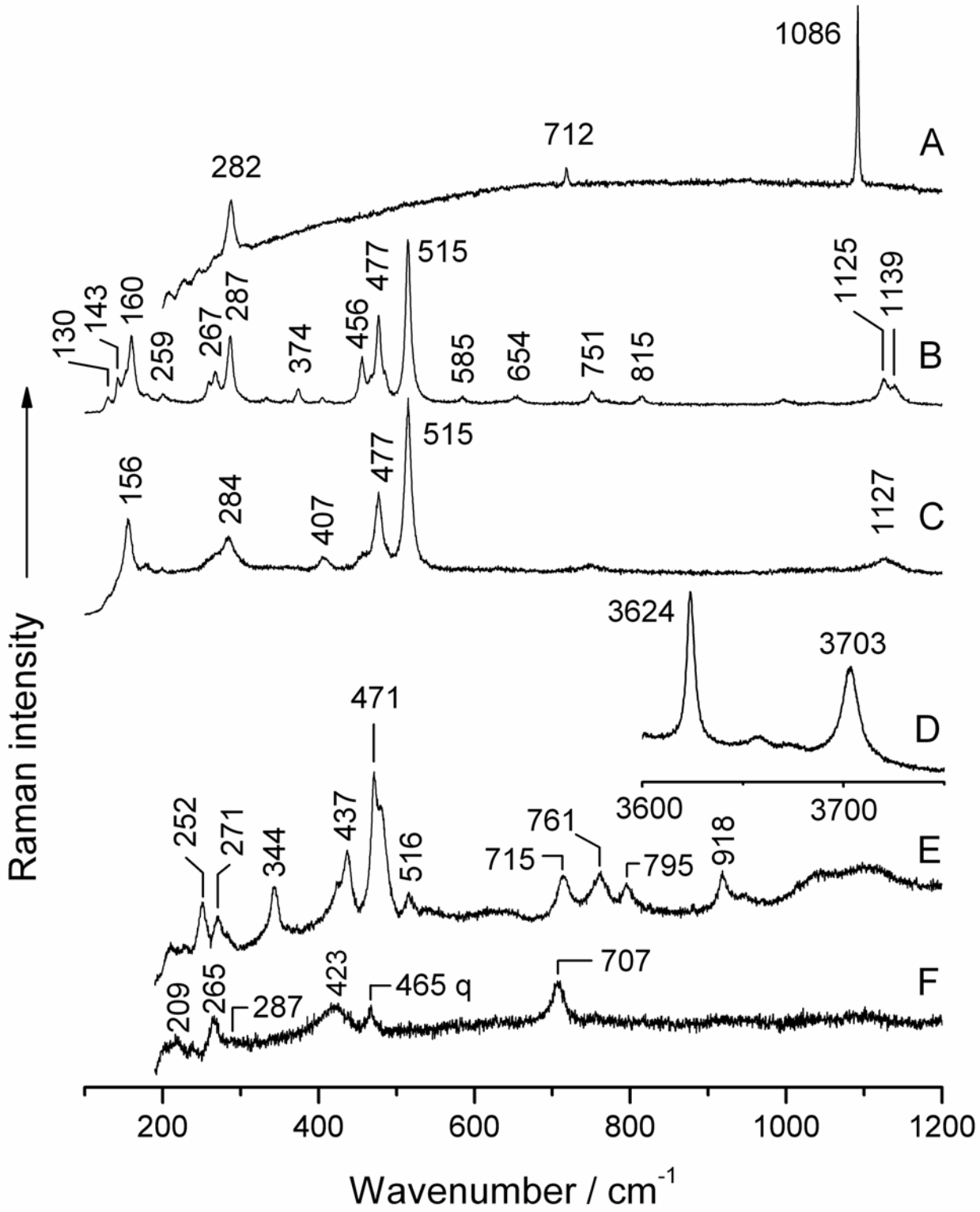
1086
712
282
A
130
143
160
259
267
287
374
456
477
515
585
654
751
815
1125
1139
B
156
284
407
477
515
1127
C
3624
3703
D
3600
3700
471
252
271
344
437
516
715
761
795
918
E
209
265
287
423
465 q
707
F
Raman intensity
200
400
600
800
1000
1200
Wavenumber / cm-1